# New aristonectine elasmosaurid plesiosaur specimens from the Early Maastrichtian of Angola and comments on paedomorphism in plesiosaurs

## R. Araújo[1,2,*], M.J. Polcyn[2], J. Lindgren[3], L.L. Jacobs[2], A.S. Schulp[4], O. Mateus[1,5], A. Olímpio Gonçalves[6] & M.-L. Morais[6]

1   Museu da Lourinhã, Rua João Luís de Moura, 2530-157 Lourinhã, Portugal

2   Huffington Department of Earth Sciences, Southern Methodist University, Daniel Avenue 75275-0395, Dallas, Texas, USA

3   Department of Geology, Lund University, Sölvegatan 12, SE-223 62 Lund, Sweden

4   Naturalis Biodiversity Center, PO Box 9517, NL-2300 RA Leiden, the Netherlands; Natuurhistorisch Museum Maastricht, De Bosquetplein 6-7, NL-6211 KJ Maastricht, the Netherlands; Faculty of Earth and Life Sciences, VU University Amsterdam, De Boelelaan 1085, NL-1081 HV Amsterdam, the Netherlands

5   Universidade Nova de Lisboa, GeoBioTec, Faculdade de Ciências e Tecnologia, 2829-516 Caparica, Portugal

6   Departamento de Geologia, Faculdade de Ciências, Universidade Agostinho Neto, Avenida 4 de Fevereiro 7, Luanda, Angola

*   Corresponding author. Email: rmaraujo@smu.edu

## Abstract

New elasmosaurid plesiosaur specimens are described from the Early Maastrichtian of Angola. Phylogenetic analyses reconstruct the Angolan taxon as an aristonectine elasmosaurid and the sister taxon of an unnamed form of similar age from New Zealand. Comparisons also indicate a close relationship with an unnamed form previously described from Patagonia. All of these specimens exhibit an ostensibly osteologically immature external morphology, but histological analysis of the Angolan material suggests an adult with paedomorphic traits. By extension, the similarity of the Angolan, New Zealand and Patagonian material indicates that these specimens represent a widespread paedomorphic yet unnamed taxon.

*Keywords*: Paedomorphism, plesiosaurs, marine reptiles, Africa, Cretaceous, histology

## Introduction

We report here new aristonectine elasmosaurid plesiosaur material from the Early Maastrichtian of Angola. Comparisons and phylogenetic analyses suggest it is closely related to and may be conspecific with an unnamed species from the Late Maastrichtian of northern Patagonia, Argentina, previously assigned to *Tuarangisaurus*? *cabazai* Gasparini, Salgado & Casadío 2003 (MML PV 5), subsequently reassigned to Plesiosauroidea indet. by Gasparini et al. (2007) and more recently to Aristonectinae gen. et. sp. indet. by O'Gorman et al. (2014). It is also indistinguishable from an unnamed taxon from New Zealand (MONZ R1526, Welles & Gregg, 1971 and

GNS CD427-429, Wiffen & Moysley, 1986). The material described here retains juvenile features in a relatively large individual. Araújo et al. (2013) and Gorman et al. (2014) reported a high proportion of 'osteologically immature' individuals in their investigated samples of elasmosaurid specimens, raising the possibility of paedomorphism in adults, a hypothesis we test through histological analysis of our material.

### Geological setting and age

Strganac et al. (2014) reported the carbon isotope stratigraphy, magnetostratigraphy and $^{40}Ar/^{39}Ar$ dates for the section at Bentiaba, Angola, which ranges in age from Cenomanian to Late

Maastrichtian. Mateus et al. (2012) summarised the amniote fauna, reporting three plesiosaur taxa from that locality. Two of the three plesiosaur taxa reported by Mateus et al. (2012) are found in the so-called Bench 19 interval, in which the majority of vertebrate fossils are concentrated (Strganac et al., 2015a), including the plesiosaur taxon described herein and a second elasmosaurid described in Araújo et al. (2015). The interval falls within magnetochron C32n.1n and is thus placed in a chronological bin approximately 240 ka in duration (71.64–71.40 Ma; Strganac et al., 2015a,b). The sediments of the Bench 19 interval are immature feldspathic sand derived from nearby granitic shield rocks, deposited on a narrow shelf at approximately 24°S paleolatitude in waters between 50 and 100 m in depth (Strganac et al., 2015a) and 18°C paleotemperature (Strganac et al., 2015b). The early Maastrichtian age of the specimens described here is biochronologically compatible with that of the New Zealand and South American aristonectine material summarised by Otero et al. (2012), but the Angola specimens mark the northernmost occurrence of an aristonectine elasmosaurid and extend the geographic range of the Late Cretaceous Weddellian Biogeographic Province (Zinsmeister, 1979).

### Institutional abbreviations

AIM – Auckland Museum, Auckland, New Zealand; BMNH – The Natural History Museum, London, UK; GNS – Geological National Survey (New Zealand), Lower Hutt, New Zealand; MGUAN – Museu de Geologia da Universidade Agostinho Neto, Luanda, Angola; MML – Museo Municipal de Lamarque, Río Negro, Argentina; MONZ – Museum of New Zealand, Te Papa Tongarewa, Wellington, New Zealand; QMF – Queensland Museum, Brisbane, Australia.

## Material and methods

### Materials

Plesiosaur specimens MGUAN PA85 (Fig. 1), MGUAN PA120 (Fig. 2), MGUAN PA248 (Figs 3 and 4) and MGUAN PA250 (Fig. 5), collected by Projecto PaleoAngola in 2007 and 2010 from Bentiaba, Namibe. The specimens are temporarily housed in the Shuler Museum of Paleontology (SMU) and Museu da Lourinhã (Portugal) but will be transferred to the Museu de Geologia da Universidade Agostinho Neto (MGUAN) collections at a later date.

### Histological procedures

Two isolated propodials from Angola (femur of MGUAN PA85 and a possible humerus MGUAN PA550) were moulded and cast prior to sampling. Transverse sections approximately 5 mm thick were removed using a diamond saw. The larger and more complete of the two elements (MGUAN PA85) was sampled at mid-diaphyseal and metaphyseo-diaphyseal height but only the metaphyseo-diaphyseal region was examined in MGUAN PA550. The samples were vacuum-embedded in polyester resin (Araldit DBF from ABIC Kemi®) to prevent shattering during slide preparation. Once embedded, one approximately 1 mm thick cross-section was cut from each block. The sections were attached to petrographic slides with polyester resin and ground to optical translucency. The cross-sections were imaged using a SONY 200 digital camera with a Tamron SPAF 90 mm macro lens and a Nikon DS-Fi1 camera attached to a binocular microscope. The osteohistological terminology follows that of Wiffen et al. (1995).

### Phylogenetic analysis

We employed the data matrix of Benson & Druckenmiller (2014), which included 270 characters and 81 operational taxonomic units (OTUs) to which we added the Angolan taxon reported here and another apparently closely related form from New Zealand (MONZ R1526 and GNS CD427-429). Two separate analyses were performed, one with the Angolan and New Zealand forms coded as individual OTUs and a second analysis with all specimens combined as a single unit to increase character coverage (see Appendix 1). The analyses were performed using TNT 1.1 (Dec 2013 version; Goloboff et al., 2008) using the 'fuse' search algorithm. The group supports were calculated using absolute and relative Bremer support (Goloboff & Farris, 2001) by TBR-swapping the trees found, keeping note of the number of steps needed to lose each group. Resampling was done by calculating the frequency and frequency differences (Goloboff et al., 2003) with 100 replications of symmetric resampling (Goloboff et al., 2003), in which each matrix was analysed with a single random addition sequence and TBR, and then collapsing the resulting tree with TBR (Goloboff & Farris, 2001). During the calculation of the strict consensus the branches with no possible support were collapsed ('rule 3'). See Appendix 1 for the taxon/character matrix.

## Systematic paleontology

Sauropterygia Owen 1860
Plesiosauria de Blainville, 1835
Elasmosauridae Cope 1869 (sensu Ketchum & Benson, 2010)
Aristonectinae Otero, Soto-Acuna, and Rubilar-Rogers, 2012
Aristonectinae gen. et. sp. indet.

*Referred specimens:* MGUAN PA85 (Fig. 1), a series of 13 cervical and dorsal vertebrae with dorsal and pectoral ribs

*Fig. 1. Aristonectinae indet. A. MGUAN PA85 in distal (1), dorsal (2) and preaxial or postaxial (3) views. 4. Ventral view. 5. Preaxial or postaxial view (distal epiphysis on top). B. Cervical and pectoral vertebrae and ribs in lateral view.*

and a partial femur; MGUAN PA120 (Fig. 2), one ischium, one femur, six autopodial elements and two sacral ribs; MGUAN PA248 (Figs 3 and 4), two autopodial elements, one phalanx, two partial coracoids, partial propodial, two neural arches and five cervical and one pectoral centra; MGUAN PA250 (Fig. 5),

two coracoids, two humeri, two vertebral centra and rib fragments.

*Locality and horizon:* Bentiaba, Angola, Mocuio Formation; from the Bench 19 interval dated at approximately 71.5 Ma (Strganac et al., 2015a).
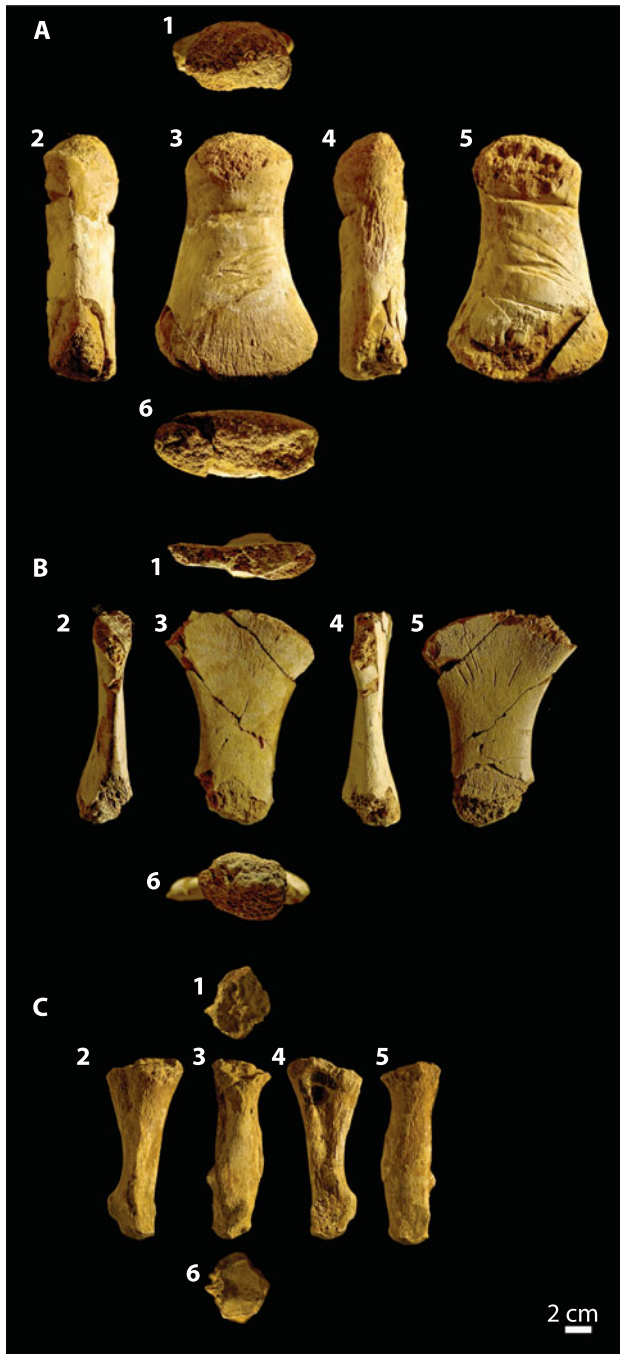
Fig. 2. *Aristonectinae indet. A. MGUAN PA120, right femur in proximal (1), preaxial (2), ventral (3), postaxial (4), dorsal (5) and distal (6) views. B. Right ischium in medial (1), posterior (2), ventral (3), anterior (4), dorsal (5) and lateral (6) views. C. Left sacral rib in medial (1), anterior (2), ventral (3), posterior (4), dorsal (5) and lateral (6) views.*

## Osteological description and comparisons

### Cervical and pectoral vertebrae

The Angolan specimen MGUAN PA248 (Fig. 3) has an anterior cervical centrum with the neural arch, but a comparable anterior centrum is seen in the New Zealand specimen MONZ

R1526 (Fig. 6, Appendix 2). The cervical centrum can only be distinguished from the pectoral centrum due to the relative position of the rib facet, higher on the pectoral (see Sachs et al., 2013). Although all centra present a shallow depression in the centre of the articular facets, the centra are effectively platycoelous. The vertebrae are wider than high and higher than long (W > H > L). The lateral sides are shallow and concave, and the ventral sides are flat. There is no evidence of a lateral keel. In anterior and posterior views, a shallow ventral and dorsal notch on the articular facets is reminiscent of the binocular-shaped vertebrae of other elasmosaurids (e.g. *Kaiwhekea*). The ellipsoidal foramina subcentralia are separated by a thick rounded ridge. The dorsal sides of the vertebrae have a concave medial region (which formed the floor of the neural canal) comprising about one-third of the dorsal area. This area is perforated by two ellipsoidal foramina that are separated by a sharp ridge. Laterally, the articular surface for the neural arch forms a crater-like D-shaped region, which is bounded by distinct edges. The rib facets are also single crater-like structures formed by ellipsoidal depressions with the long axis parallel to the anteroposterior axis of the centra. Two neural arches are preserved; one is missing one pedicle and the apex of the neural spine and the other comprises only the neural spine. The pedicle is thick at the base, becomes very thin in the middle and then expands to meet the neural spine. In ventral view, the articular surface with the centrum is roughened and oval. In the posterior part of the pedicle, at the junction with the neural spine, there is a small foramen. The prezygapophyses are proportionally small relative to the centra and form a rounded cup with no separation between the two. The prezygapophyses protrude at a high angle to the vertical plane (~70°). The surface of the prezygapophyses is roughened. The dorsal edge of the prezygapophyses extends to the neural spine about one fifth its length in the form of a crest. The connection of the prezygapophyses to the neural spine is a smooth upwards curve. In anterior view, the base of the neural spine is pierced by two teardrop-shaped foramina. The postzygapophyses are in contact with each other, although at the intersection there is a shallow depression between them. The neural spine borders are straight and sub-parallel to each other. At mid-height, the anterior border is pierced by an elongated foramen, and the posterior border is excavated by an elongate slit.

The cervicals preserved in MGUAN PA85 (Fig. 1B) represent a more posterior position than those of MONZ R1526 (Fig. 6A) and MGUAN PA248 (Fig. 3). The cervicals do not increase significantly in length posteriorly. Also, the vertebral width does not increase significantly relative to their length. The length of the centra is consistently less than is the height. The articular surfaces of the cervical centra are markedly elliptical with the short axis corresponding to the height. Cervical centra are concave laterally and slightly amphicoelous. The cervical centra have slightly concave articular facets in some vertebrae and do not present the binocular-shape as in other species
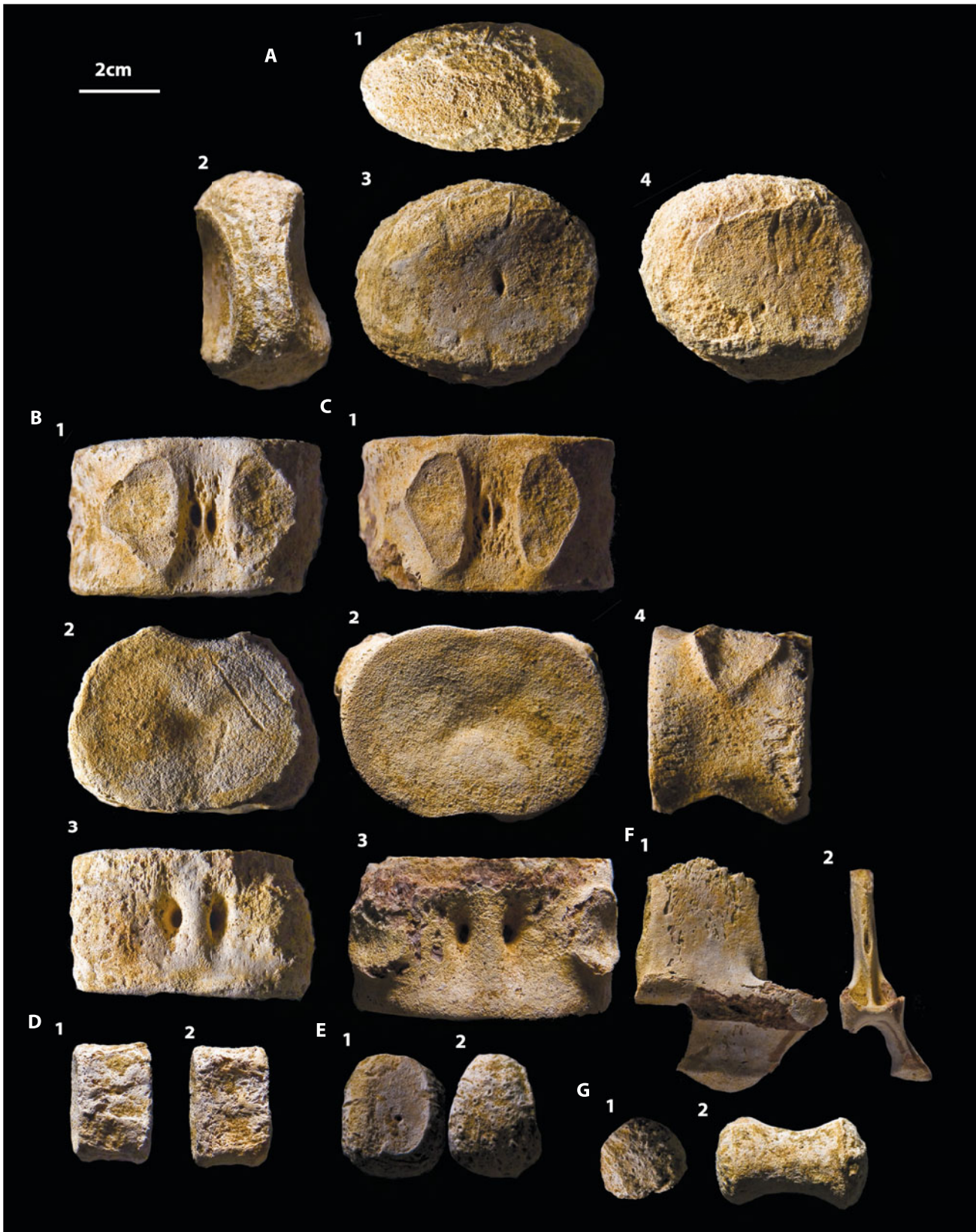
Fig. 3.  *Aristonectinae indet. MGUAN PA248. A. Mesopodial element in proximal (1), postaxial (2), dorsal (3) and ventral (4) views. B. Cervical centrum in dorsal (1), anterior (2) and ventral (3) views. C. Pectoral centrum in left lateral (1), anterior (2), right lateral (3) and ventral (4) views. D. Posterior caudal vertebra (?) in dorsal (1) and ventral (2) views. E. Distal mesopodial element in dorsal (1) and ventral (2) proximal views. F. Cervical neural arch in lateral (1) and anterior (2) views. G. Autopodial element in proximal (1) and distal, preaxial, postaxial, dorsal or ventral (2) views.*

Fig. 4. *Aristonectinae indet. MGUAN PA248. A. Posterior cervical centrum in dorsal (1), left lateral (2), anterior (3), right lateral (4) and ventral (5) views. B. Posterior cervical centrum in anterior (1), ventral (2) and lateral (3) views. C. Posterior cervical centrum in left lateral (1), anterior (2), right lateral (3) and ventral (4) views. D. Left humerus dorsal (1), postaxial (2), proximal (3), ventrsal (4), preaxial (5) and distal (6) views. E. Cervical neural arch in dorsal (1), lateral (2) and ventral (3) views. F. Right coracoid fragment in ventral (1), medial (2) and dorsal (3) views. G. Right coracoid fragment in ventral (1), medial (2) and dorsal (3) views.*

(e.g. *Kaiwhekea*, Cruickshank & Fordyce, 2002). The vertebrae are from the posterior portion of the neck because they are flat (Sato, 2005) and do not have a cylinder-like, gentle restriction on the adjacent vertebral facets (Carpenter, 1996; Williston, 1903). Furthermore, there are no lateral or ventral keels on the cervical vertebrae, indicative of a posterior position (Sato, 2002). The articular facets for the ribs are sub-circular and single-headed. There is a well-defined protruding rim for the rib articulation. The pectoral centra can be identified by possessing functional rib facets transected by the neurocentral suture (Sachs et al.,

2013). In the pectoral centra, the areas of attachment for the neural spine form a lateral bump, and in dorsal view a D-shaped area of articulation (Fig. 1B). The area of attachment for the neural spine is not visible in the cervical centra. The foramina subcentralia are present in the cervical and pectoral vertebrae. These foramina are situated far apart from each other in the cervical centra. Some pectoral vertebrae bear a maximum of six foramina subcentralia. The widely separated foramina are shared by cryptocleidoids (O'Keefe & Street, 2009), but are also visible in posterior cervical vertebrae of *Dolichorhynchops osborni* (Williston, 1903).
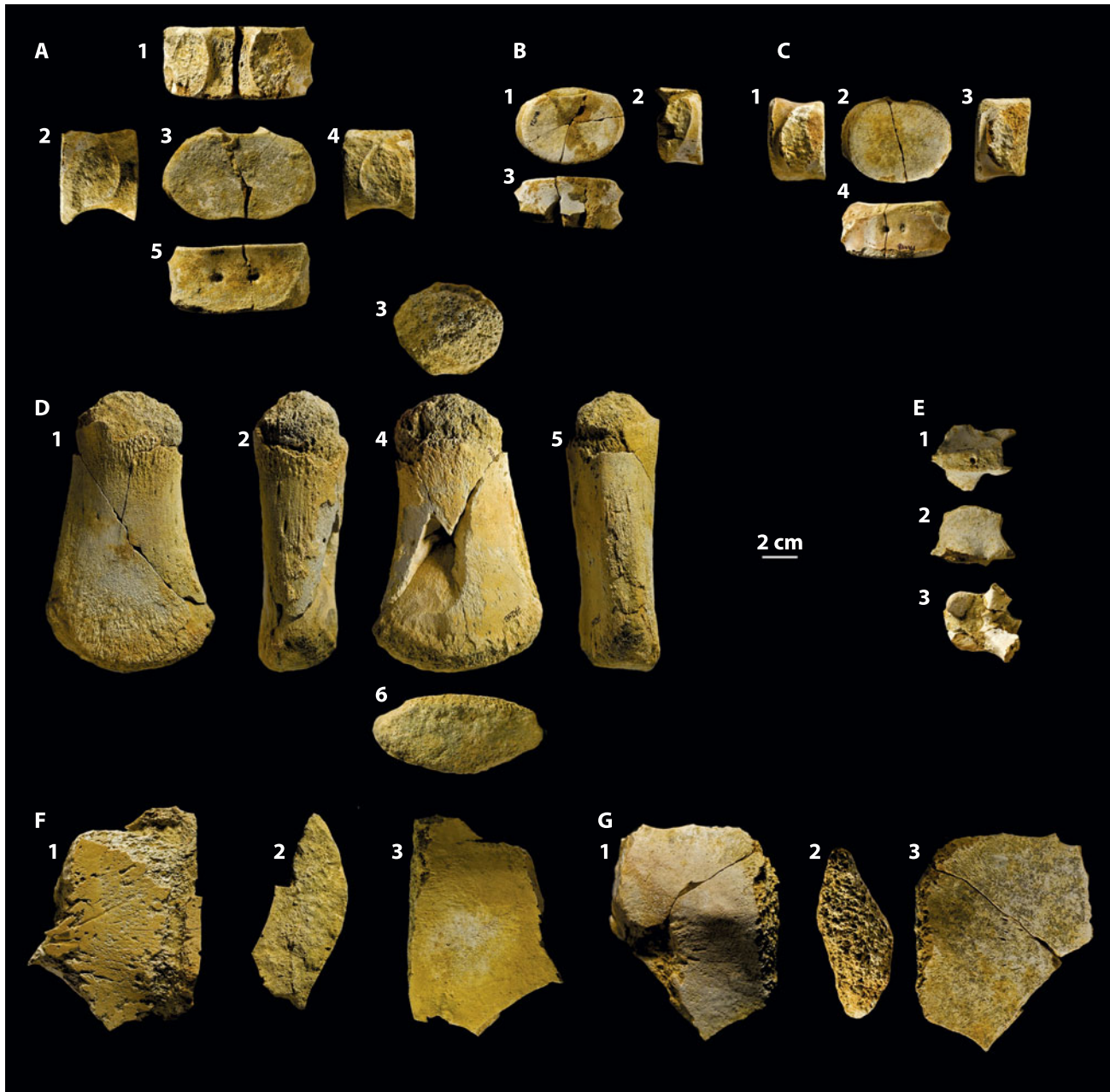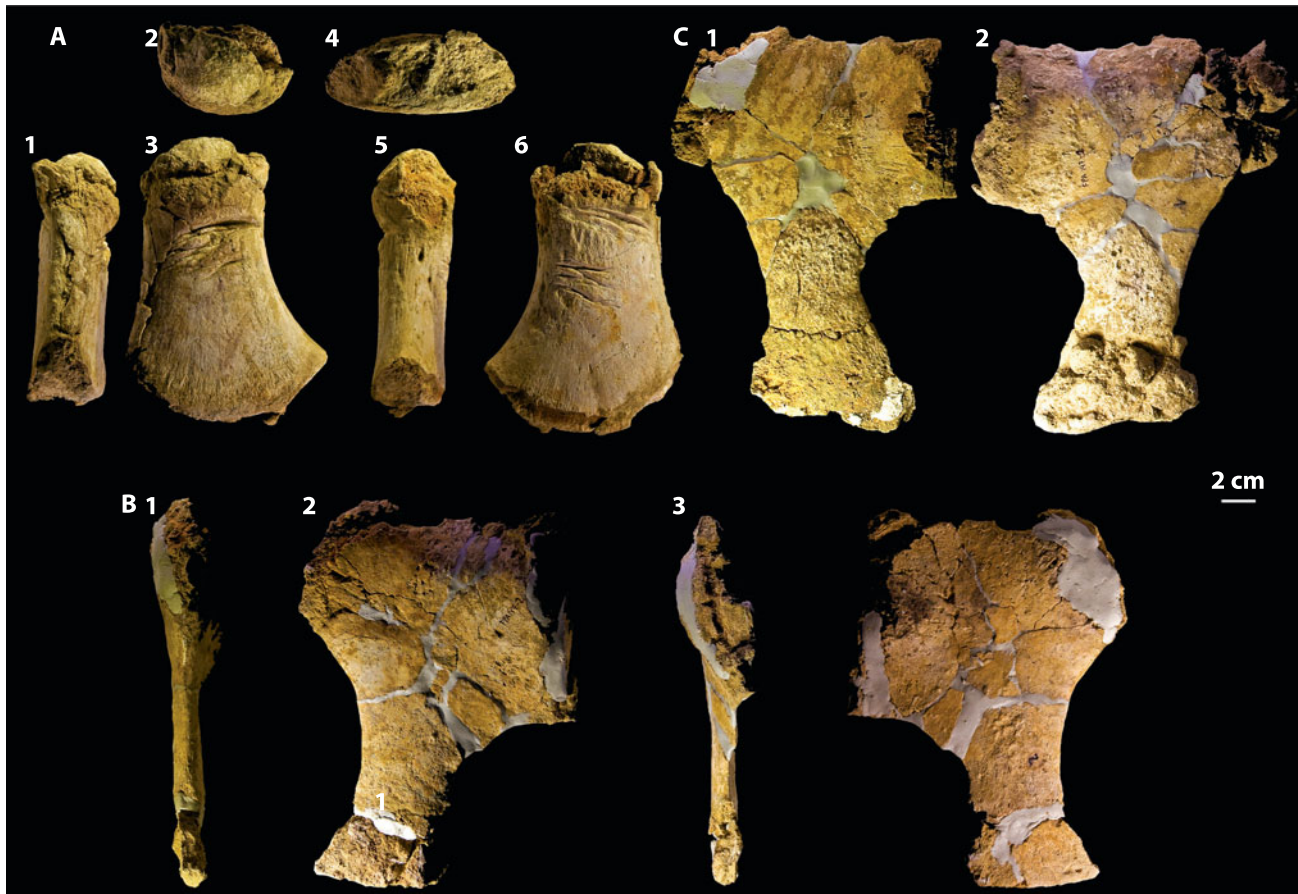
*Fig. 5. Aristonectinae indet. MGUAN PA250. A. Left humerus in preaxial (1), proximal (2), dorsal (3), distal (4), postaxial (5) and ventral (6) views. B. Left coracoid in lateral (1), dorsal (2), medial (3) and ventral (4) views. C. Right coracoid in ventral (1) and dorsal (2) views.*

In addition to the ventral foramina, there are two elliptical dorsal foramina edged laterally and medially by two ridges; the median ridge only extends along the side of the foramina. Pedicles are thinnest halfway from the centrum to the neural spine. The neural spines are straight (i.e. not angled posteriorly), compressed and blade-like; as opposed to those seen in pliosaurids such as *Macroplata* (White, 1940) or in the rhomaleosaurid *Stratesaurus* (Benson et al., 2012). The apex of the neural spine is slightly rounded or flat and there is no swelling of the neural spine apex as in the elasmosaurid *Futabasaurus* (Sato et al., 2006). The neural spine is slightly concave along the posterior border, producing a small space between neural spines for relative movement; the apex actually touches the adjacent neural spines. In the cervicals the prezygapophyses are conjoined yet distinct, but in the pectorals they are fully separated. The pre- and postzygapophyses are narrower than the centrum, and the zygapophyses are nearly horizontal. The zygapophyseal angle along the cervical vertebral series remains constant. The prezygapophysis dorsal surface is markedly concave whereas that of the postzygapophysis is flat. There is a slight ridge extending posteriorly from the prezygapophysis.

The dorsals preserved in MGUAN PA85 are in all respects very similar to those of MONZ R1526 (Fig. 6) and MML-PV5 (O'Gorman et al., 2014). In MONZ R1526 (Fig. 6B) only the neural spines and the transverse processes are visible on the sequence of dorsal vertebrae (Fig. 6, central line drawing). In the dorsal vertebral centrum detached from the specimen block MGUAN PA85, as in MONZ R1526, the neural spines are short and thick lateromedially, bear straight or slightly concave anterior and posterior borders, and are well separated from the adjacent neural spines. The apex of the neural spines is smoothly convex in lateral view. The transverse processes arise from the anterior portion of the pedicles and are very stout and cylindrical; the rugose articular facet is flat or slightly convex. The dorsal centrum closely resembles that of MML-PV5 (Gasparini et al., 2003; O'Gorman et al., 2014) and GNS CD429 (Fig. 7C; Wiffen & Moisley, 1986); it is characteristically wide, giving an ellipsoidal shape to the sub-platycoelous anterior and posterior articular facets. The attachment area for the neural arch is sub-circular and expands slightly beyond the sides of the centrum. The neural canal carves a shallow gutter that is pierced by two anteroposteriorly elongated foramina, which in the preserved vertebrae are all in the same relative position in the centra.

### Ribs

In MGUAN PA85 (Fig. 1B) and MGUAN PA248, as well as in MONZ R1426 (Fig. 6, central line drawing), the dorsal ribs are gently
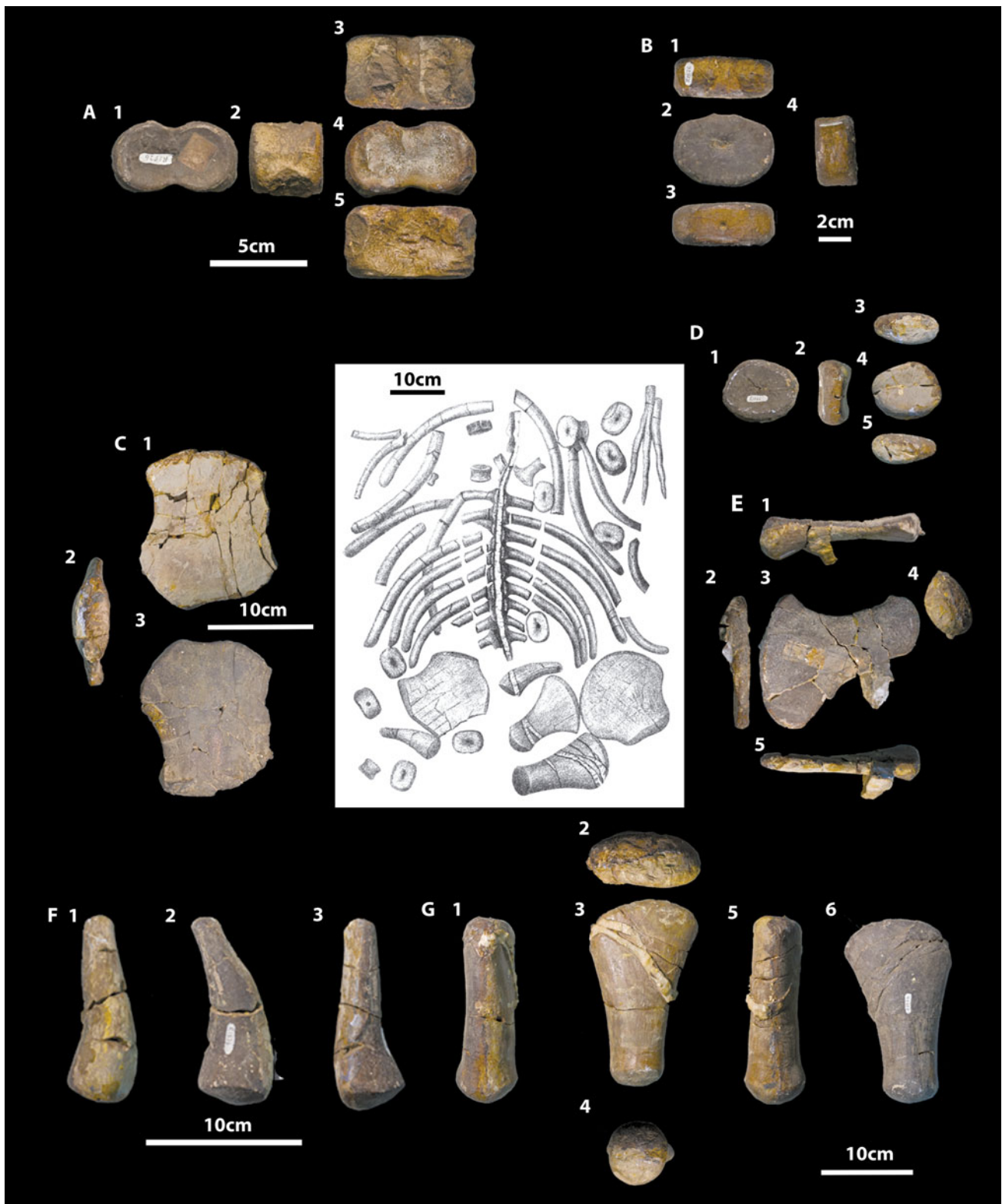
Fig. 6. *MONZ R1526, previously referred to 'Plesiosaurus australis' by Hector (1874). A. Anterior cervical vertebral centrum in anterior (1), lateral (2), dorsal (3), posterior (4) and ventral (5) views. B. Dorsal vertebral centrum in dorsal (1), anterior or posterior (?) (2), ventral (3) and lateral (4) views. C. Pubis in ventral (1), acetabular (2) and dorsal (3) views. D. Mesopodial element: ventral or dorsal views (1 and 4), preaxial or postaxial view (2), proximal or distal views (3 and 5). E. Right ischium in posterior (1), medial (2), dorsal (3), acetabular (4) and anterior (5) views. F. Left ilium in anterior (1), medial (2) and posterior (3) views. G. Right femur in preaxial (1), distal (2), dorsal (3), proximal (4), postaxial (5) and ventral (6) views.*

*Fig. 7. GNS CD427–429, previously referred to 'juvenile' cf.* Tuarangisaurus keyesi *by Wiffen & Moisley (1986). A. GNS CD428 coracoid and scapula in coracoid in medial (1), scapula in dorsal (2) and coracoid in lateral (3) views. B. GNS CD428 coracoid in lateral (1), anterior (2), ventral (3), medial (4) and*

curved and cylindrical. In MGUAN PA85 there are six ribs, which are most probably pectoral ribs due to the robustness and taphonomic location. However, there is an isolated dorsal rib overlying the vertebrae in the cervical-pectoral transition. Pectoral ribs have a capitulum and tuberculum, contrary to the dorsal ribs (see also Sachs et al., 2013). The pectoral rib is sub-circular in cross-section, although a slight groove is present on the anterior and posterior sides. There is a sacral rib preserved in MGUAN PA120 (Fig. 2C). The medial heads of the sacral rib are heavily pitted and rugose, the lateral head is smooth. The medial head is roughly D-shaped, and it has two facets with two different orientations and the faint line that separates them is oriented anteroposteriorly. The dorsal border is slightly concave and the ventral border is more strongly concave. There are two processes: one distal on the ventral border and another anteriorly projecting. In dorsal view, the posterior border is sinusoidal and the anterior border is straight with the exception of the process.

### Scapulae

Thus far a scapula has not yet been collected from the early Maastrichtian of Angola, but some material from New Zealand that is indistiguishable from Angolan material comprises overlapping material, and therefore we describe the New Zealand portions as a proxy for those not present in the Angolan material. A nearly complete scapula (AIM LH1521) has a broad base for the dorsal process and is very similar to GNS CD428, but the tip of the dorsal process is missing. The articular portion is slightly concave, highly rugose and pitted, bearing a coracoidal and glenoid facets. The glenoid in AIM LH1521 is slightly convex and without any articular facets, and differs from the condition of GNS CD428 (Fig. 7A and E), but may be due to ontogeny. The dorsal process has a broad straight base and tapers dorsally, being crushed dorsoventrally in GNS CD428 (Fig. 7A and E). The tip of the dorsal process of AIM LH1521 points slightly posteriorly. The median portion of the ventral plate of the scapula is missing. The preserved anteroposterior length of AIM LH1521 is 13.9 cm.

### Coracoids

MGUAN PA250 (Fig. 5) preserves two coracoids with complete posterior borders, although the medial and lateral portions are partially damaged and compare well with GNS CD428 (Fig. 7A and E) and MML-PV5 (O'Gorman et al., 2014). The coracoids are composed of the thickened and subrectangular glenoidal portion that expands into the posterior process. The anterior border is slightly concave. The glenoid border is straight and forms an angle with the lateral border of the posterior process, but there are no clearly defined glenoid and scapular facets. The posterior border is straight and nearly half the size of the anterior border. The intercoracoid vacuity is formed by a deep subcircular excavation of the medial border of the posterior process. The intercoracoid symphysis articulation is straight. The ventral buttress of the coracoid is small ($\sim$1 cm) and semi-conical, arising from the midpoint of the intercoracoid symphysis (e.g. also known in *Syxosaurus*, *Woolungasaurus* or *Wapuskanectes*; Welles & Bump, 1949; Sachs, 2004; Druckenmiller & Russell, 2006). The dorsal and ventral surfaces of the coracoids are rugose, particularly near the posterior process, possibly as a result of muscle attachment. There is no evidence of the posterior cornua of the coracoids (i.e. lateral projection on the posterior border of the coracoids) or preglenoid processes (i.e. anterior projection on the medial intercoracoid symphysis). In MGUAN PA248 (Fig. 4F and G), the preserved coracoid portions comprise the intercoracoid symphysis. The ventral buttress is semicircular in medial view.

### Humerus

The best preserved humeri are from MGUAN PA250 (Fig. 5A) and MGUAN PA248 (Fig. 4D), but very similar humeri are present in the New Zealand and Argentine collections (e.g. AIM LH1519, MML-Pv5). These elements are identified as humeri because in many plesiosaurs the humerus is typically more distally asymmetrical than the femur (Gasparini et al., 2003). In these specimens the humerus possesses a well-marked postaxial angle between the articular facet and the postaxial edge. Additionally, the pre- and postaxial edges of the humerus tend to be more curved that in the femur (see also Gasparini et al., 2003). The humeri in MGUAN PA250 and MGUAN PA248 are massive and short elements (W/L average ratio 0.76). The proximal epiphysis, although partially damaged in MGUAN PA250, is hemispherical and covered by small (0.2–0.5 cm) conical structures that occasionally anastomose with each other. These structures are probably vascular canals and not unfinished cancellous bone on the articular surfaces of the propodial. The distal end of the humerus is convex and there are no distinguishable epipodial facets for the radius and ulna. The distal end is oval in cross-section, with the dorsal border being slightly more convex than the ventral border. The dorsal

*dorsal (5) views. C. GNS CD427 dorsal vertebrae sequence in ventral (1), posterior (2), lateral (3) and dorsal (4) views. D. GNS CD427 paddle. E. GNS CD428 scapula in lateral (1), medial (2), anterior (3), dorsal (4) and glenoidal (5) views. F. GNS CD429 pubis in acetabular (1), dorsal (2) and anterior (3) views. G. GNS CD429 dorsal neural arch in ventral (1), anterior (2) and lateral (3) views. H. GNS CD429 ischium in anterior (1), glenoidal (2), ventral (3) and medial (4) views. I. GNS CD428 humerus in preaxial or postaxial (1), proximal (2), dorsal or ventral (3) and distal (4) views. J. GNS CD429 dorsal vertebral centrum in lateral (1), dorsal (2), anterior or posterior (?) (3) and ventral (4) views.*

and ventral sides of the humerus are heavily marked by serrations perpendicularly oriented to the proximodistal axis of the bone. These are apparently bite marks, probably caused by *Squalicorax pristodontus* due to the size, serration pattern and the presence of secondary lineations perpendicular to the main grooves (Schwimmer et al., 1997; Shimada et al., 2010). *Squalicorax pristodontus* is also the most common shark at the locality, represented by shed teeth associated with most

amniote carcasses (Strganac et al., 2015a). The surface of the ventral and dorsal borders is striated on the distal end by shallow subparallel slits. The preaxial border is nearly straight whereas the postaxial border is concave, forming a distinct kink with the distal border. The whole extent of the preaxial border is covered with muscle scars. On the postaxial border there is a 1.5 cm foramen in the diaphysis but closer to the proximal end. In MGUAN PA550 (Fig. 8) the propodial element is very
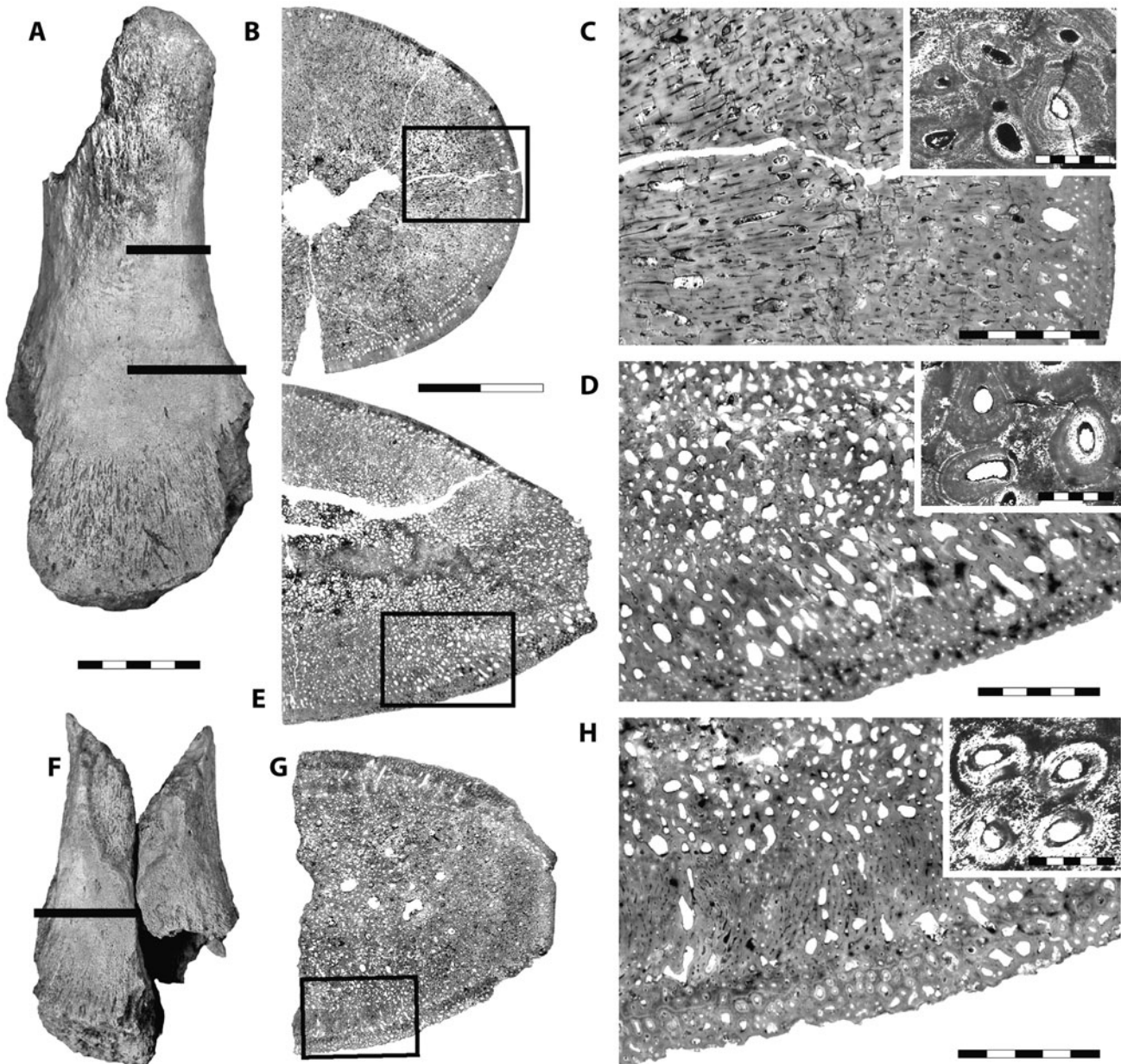


Fig. 8. *Aristonectinae indet.* Bone histology of specimens MGUAN PA85 and MGUAN PA550, two isolated propodials. A–E. MGUAN PA85. A. The bone prior to osteohistological analysis. The areas from which the mid-diaphyseal and metaphyseo-diaphyseal sections were taken are marked with horizontal bars. B. Mid-diaphyseal section. C. Close-up of the area marked in B. Inset shows secondary osteons from the cortical region of the bone surrounded by remains of globular calcified cartilage. D. Metaphyseo-diaphyseal section. E. Close-up of the area marked in D. Inset shows secondary osteons from the cortical region of the bone surrounded by remains of globular calcified cartilage. F–H. MGUAN PA550. F. The bone prior to osteohistological analysis. The area from which the metaphyseo-diaphyseal section was taken is marked with a horizontal bar. G. Metaphyseo-diaphyseal section. H. Close-up of the area marked in G. Inset shows primary osteons from the cortical region of the bone surrounded by globular calcified cartilage. Scale bars represent 5 cm (A, F), 2 cm (B, D, G), 5 mm (C, E, H) and 500 μm (inset in C, E, H).

fragmentary; only the proximal portion is preserved and it is difficult to discern whether it is a femur or humerus. The head of the propodial is hemispherical, and, from what is preserved, is apparently a short, massive bone.

### Autopodials

In both MGUAN PA120 (Fig. 2) and MGUAN PA248 (Fig. 3A, E and G), the autopodial elements are discoid and sub-circular with some degree of ellipsoidal eccentricity, thus belonging to the mesopodium or epipodium. They have a cap of periosteal bone on the dorsal and ventral sides bearing randomly placed foramina. On the remainder of the surface the trabecular structure of the bone is visible. The phalanx is hourglass-shaped; the proximal and distal borders are convex, and it is pierced by several irregularly located foramina. The proximal and distal facets are perforated by several equally-spaced conical structures.

### Pubis

There is no pubis collected thus far from Angola, but the pubis in MONZ R1526 (Fig. 6C) is subcircular, flat and dorsoventrally thick as in MML-PV5 (Gasparini et al., 2003; O'Gorman et al., 2014) and GNS CD429 (Fig. 7F, Wiffen & Moisley, 1986). Likewise, the excavation for the pelvic fenestrum is gently concave. The ogival to ellipsoidal acetabular region is convex and slightly rugose. A minor anterior excavation forms the short constriction for the acetabulum. Although slightly damaged, the acetabular region is unfaceted.

### Ischium

A single ischium from Angola was collected in MGUAN PA120 (Fig. 2B). It is comparable to MONZ R1526 (Fig. 6E), as in MML-PV5 (O'Gorman et al., 2014), and GNS CD429 (Fig. 7H). The ischium is flat except on the thickened acetabular portion. The anterior and posterior borders are gently concave, whereas the medial border is convex. The shallow concavities of the pubic posterior border and the ischial anterior border form an ellipsoidal pelvic fenestra. Medially, the anterior angle is sharper than the rounded posterior angle of the ischium and bears several grooves in MGUAN PA120. The posterior projection of the ischium is short. The acetabular portion is oval and convex, bearing a rugose pattern, and anteriorly there is a small facet for the articulation of the pubis. The lateral head is ellipsoidal and fans laterally. The ischia have an anteromedial edge forming a right angle and the contour of the medial border is almost uniformly convex.

### Ilium

No ilium was collected from Angola. In MONZ R1526 (Fig. 7F) and MML-PV5 (O'Gorman et al., 2014) the ilium is conical but kinked with an elongated ovoid dorsal tip and hemispherical ventral articular surface. The dorsal articular surface is smoothly convex and the transition towards the more ventral portion of the ilium is smooth. The ventral articular shape is convex with a marked edge for the more dorsal portion of the ilium. The shape of the MONZ R1526 (Fig. 7F) ilium differs significantly from other Late Cretaceous elasmosaurid plesiosaur taxa (e.g. *Thalassomedon, Terminonatator, Futabasaurus*; Welles, 1943; Sato, 2003; Sato et al., 2006) because of its simple conical but kinked shape. The ilia described here are not twisted.

### Femur

The femora of MGUAN PA120 (Fig. 2A) and MGUAN PA85 overlap morphologically with MONZ R1526 (Fig. 6G), GNS CD427 (Fig. 7I) and MML-PV5 (O'Gorman et al., 2014). The femur is robust, with an unfaceted, flattened distal epiphysis and the proximal end is sub-circular in articular view. The postaxial and preaxial borders are sub-parallel proximally and diverging distally, producing a slightly expanded epiphysis anteroposteriorly. The hemispheric proximal articular facet is faintly delineated. No trochanter is present. Both the proximal and distal epiphysis bear striated rugosities for muscular attachment that are proximodistally oriented, especially in MGUAN PA120 (Fig. 2A). In the distal epiphysis the striations cover about one fifth of the length of the femur. The striated zone can be divided into a proximal zone (mostly composed of pits that furrow proximally), an intermediate zone (composed of deep striations) and a distal zone (defined by the hints of either striae or pits). On the anterior and posterior sides there are extensive areas with muscle scars; one of the sides bears long sub-parallel grooves ridges. The proximal and distal epiphyses are intensely covered by small crater-like structures about 0.3 cm in diameter.

The elongation ratio (i.e. distal width divided by proximodistal length) is indicative of elasmosaurid affinities assuming isometric growth: $12.3 \div 17.7 = 0.69$. The elongation ratio is 0.46 in the plesiosaurid *Plesiosaurus dolichodeirus* (Storrs, 1995), 0.46 in the rhomaleosaurid *Rhomaleosaurus cramptoni* (Smith, 2007), 0.52 in the polycotylid *Trinacromerum ?bentonianum* (Albright et al., 2007), 0.53 in the polycotylid *Eopolycotylus rankini* (Albright et al., 2007), 0.60 in the elasmosaurid *Terminonatator herschlensis* (Sato, 2003), 0.66 in the elasmosaurid *Thalassomedon haningtoni* (Welles, 1943), 0.68 in the elasmosaurid *Mauisaurus haasti* (Hiller et al., 2005) and 0.63 in MGUAN PA85 (Fig. 1A). The femur is a massive bone lacking part of the proximal and distal epiphyses. The distal epiphysis does not have facets, the shaft is straight, the anterior and posterior facets are equally concave. The distal epiphysis seems to be ellipsoidal. Both the proximal and distal portions of the shaft have a high density of muscle scars.

### Results of phylogenetic analysis

Analysis with all specimens combined in a single OTU produced 112 MPTs, after 343,394,314 rearrangements, with the best tree

length of 1336 steps. The analysis with the Angolan and New Zealand material run as separate OTUs produced 102 MPTs, after 356,273,327 rearrangements, also with the best tree length of 1336 steps. A portion of the strict consensus tree for both of these analyses and their support indices are shown in Fig. 9 (for the full trees see Supplementary Figures 1 and 2). The Angolan taxon was recovered as the sister-taxon to the New Zealand material (MONZ R1526 and GNS CD427-429), and those together as the sister-taxon to *Aristonectes* plus *Khaiwhekea*. Additionally, the new Angolan material described here is indistinguishable from the New Zealand (MONZ R1526 and GNS CD427-429) and South American material (MMLPV5) and may represent a single aristonectine elasmosaurid taxon (sensu O'Gorman et al., 2014).

Unequivocal characters supporting the new material as an elasmosaurid are the ratio of humerus to femur length between 0.9 and 1.1 (Benson & Druckenmiller, 2014, 241:1), and the humerus not being inclined but extending proximally so the shaft is straight (Benson & Druckenmiller, 2014, 249:1). Aristonectine characters include the proportions of anterior-middle cervical centra that are approximately as long as high (Benson & Druckenmiller, 2014, 153:1) and are united with the New Zealand material due to the V-shaped neurocentral suture in the anterior-middle cervical vertebrae in lateral view (Benson & Druckenmiller, 2014, 172:1), but is differentiated from *Aristonectes* plus *Khaiwhekea* by the presence of the lateral ridges on the lateral surfaces of anterior cervical centra (Benson & Druckenmiller, 2014, 154:1)

## Histological results and discussion

The section taken from the mid-diaphyseal region of MGUAN PA85 has high compactness, although the woven-fibered bony tissues are pierced by a dense network of primarily radiating vascular canals (Fig. 8B and C). Numerous longitudinally directed vascular canals are also present, and each canal is
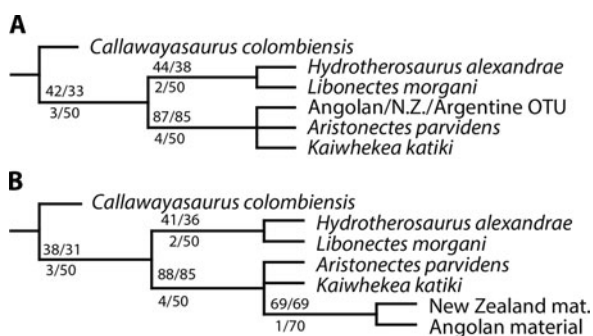


*Fig. 9. Strict consensus tree from phylogentic analysis. A. Phylogenetic tree with the Angolan, New Zealand and Argentine material merged into a single OTU. B. Phylogenetic tree with the Angolan and New Zealand material as separate OTUs. Symmetric resampling/GC values are noted above branches and absolute bremer support/relative bremer support values are noted below branches. See Supplementary Material Figures 1 and 2 for complete trees.*

surrounded by centripetally deposited bone tissue to form primary and secondary osteons. Three lines of arrested growth (LAGs) are visible and can be traced over long distances. Deeper in the cortices intense Haversian remodelling has contributed to the formation of abundant secondary osteons (Fig. 8C, inset). The vascular network of the medullary area is predominantly radial, although longitudinally directed canals occur (Fig. 8C). Centripetal deposits of pseudolamellar tissue surround the lumen of the densely packed canals. Larger erosional cavities are relatively few and randomly scattered.

The section taken at the metaphyseo-diaphysis of MGUAN PA85 (Fig. 8D and E) is conspicuously more cancellous than that taken at the mid-diaphysis (Fig. 8B and C), illustrating significant structural differences that appear locally in the appendicular bones of these derived plesiosaurs. The peripheral parts of the rather thin periosteal cortices contain three LAGs and primary osteons dispersed in an intercellular matrix composed predominantly of globular calcified cartilage. Further internally is a zone of densely packed secondary osteons with scattered remains of calcified cartilage (Fig. 8E, inset). The medullary spongiosa is composed of an intensively remodelled, plexiform meshwork of vascular canals made up of centripetally deposited pseudolamellar bone tissue interbedded with sparse remnants of globular calcified cartilage.

The metaphyseo-diaphyseal section taken from the smaller, more incomplete propodial, MGUAN PA550 (Fig. 8), is also highly cancellous with numerous irregular erosional cavities (Fig. 8G and H). The highly vascularized cortex of MGUAN PA550 is relatively thin and contains few secondary osteons, but primary osteons are abundant and interspersed randomly in an intercellular matrix composed of globular calcified cartilage and radially oriented Sharpey's fibers (Fig. 8H, inset). One LAG is discernable. The trabeculae of the medullary spongiosa are composed of a core of globular calcified cartilage covered by pseudolamellar endosteal bone. Locally, the medullary zone is occupied by dense networks of plexiform and radially oriented vascular canals separated by woven-fibred bone tissue and calcified cartilage (Fig. 8H).

Wiffen et al. (1995) concluded that plesiosaur propodials varied from a pachyostotic to osteosclerotic condition through ontogeny, a pattern more broadly recognised by Houssaye (2009; but see also Talevi & Fernández, 2014). The 'Wiffen et al. juvenile' (Wiffen et al., 1995) histological traits are congruent with the 'Brown juvenile' (Brown, 1981) external morphological traits. Following Wiffen et al. (1995) two different ontogenetic stages are recognised: (1) the 'juvenile' condition in which the humerus is pachyostotic, i.e. has a thick layer of cortical bone and the medullary zone is pierced by some erosional lacunae, and (2) the 'adult' condition in which the propodials are largely cancellous with intense Haversian remodelling, although locally bearing a relatively compact cortex.

In the Angolan specimens analysed here, the propodials have osteosclerotic histology and secondary osteons nearly to

the outermost regions of the sectioned bones. The bone is largely cancellous with intense Haversian remodelling, consistent with the 'Wiffen et al., 1995 adult' condition. The presence of three LAGs (in MGUAN PA85, Fig. 8) supports the adult condition of the specimen. Additionally, the muscle scars formed by deeply grooved and reworked periosteum are indicative of late ontogenetic stages as observed in other vertebrates (e.g. Tumarkin-Deratzian et al., 2006). This adult histological bone fabric is in contrast to the juvenile external morphology, in particular the small size, the unfaceted distal propodials, the flat articular facets of the vertebrae, the non-fusion of the neural arches with the centra, the near-absence of the posterior cornua of the coracoids and the absence of the pectoral bar, all traits congruent with the 'Brown juvenile' condition. Thus, histological and osteological data presented here for the Angolan specimen suggests it is in fact a paedomorphic adult, and by extension this may be the case in the apparently closely related specimens from Argentina (MMLPV5), as suggested by O'Gorman et al. (2014), and from New Zealand (MONZ R1526 and GNS CD427-429).

## Summary and conclusions

Only in rare cases can sexual maturity in plesiosaurs be assessed, such as the unambiguous preservation of a gravid female (O'Keefe & Chiappe, 2011). Thus, analysis of the microarchitecture of bone in conjunction with assessment of osteological maturity may be the only current approach to judge the ontogenetic maturity of an animal and the expression of paedomorphism in certain clades. In the absence of a histological analysis, the terms 'adult' or 'juvenile' become arbitrary, and we therefore recommend using the terms 'osteologically mature' or 'osteologically immature' when an osteohistological analysis is not performed.

More onerous are the affects of paedomorphism on phylogenetic analyses and taxonomic practices. Despite being a questionable taxonomic procedure (ICZN, Art. 69), numerous new genera and species have been erected using putative 'juvenile' and 'subadult' specimens (e.g. Cruickshank et al., 1996; Sato & Wu, 2006; Druckenmiller & Russell, 2008; Berezin, 2011; Ketchum & Benson, 2011; Vincent & Benson, 2012; Knutsen et al., 2012; Vincent et al., 2012), while others are now considered as *nomina dubia* due to their putative juvenile condition without critical assessment of the confounding effects of heterochrony (e.g. *Tuarangisaurus*? c*abazai* Gasparini et al., 2007 and *Leurospondylus ultimus* Brown, 1913; see also Sato & Wu, 2006). For example, *Leurospondylus ultimus* has been systematically ignored in phylogenetic analysis because it is thought to be a juvenile.

We have shown through the use of histological analysis that the osteologically immature specimens from Angola reported here are paedomorphic adults. Moreover, we have presented evidence that similar specimens from New Zealand and Argentina most probably belong to the same, as yet unnamed, taxon.

## Supplementary Material

## Acknowledgments

## References

**Albright, L.B., III, Gillette, D.D. & Titus, A.L.**, 2007. Plesiosaurs from the Upper Cretaceous (Cenomanian-Turonian) Tropic Shale of southern Utah, part 2: Polycotylidae. Journal of Vertebrate Paleontology 27: 41-58.

**Araújo, R., Lindgren, J., Jacobs, L., Polcyn, M. & Schulp, A.**, 2013. Phylogeny and paedomorphism in Angolan Maastrichtian elasmosaurids. Journal of Vertebrate Paleontology, Program and Abstracts 79.

**Araújo, R., Polcyn, M.J., Schulp, A.S., Mateus, O. & Jacobs, L.L.**, 2015. A new elasmosaurid from the early Maastrichtian of Angola and the implications of girdle morphology on swimming style in plesiosaurs. Netherlands Journal of Geosciences. 12p. doi: 10.1017/njg.2014.44.

**Benson, R.B.J. & Druckenmiller, P.S.** 2014. Faunal turnover of marine tetrapods during the Jurassic-Cretaceous transition. Biological Reviews 89: 1-23.

**Benson, R.B.J., Evans, M. & Druckenmiller, P.S.**, 2012. High diversity, low disparity and small body size in plesiosaurs (Reptilia, Sauropterygia) from the Triassic-Jurassic boundary. PLoS ONE, 7, e31838. doi:10.1371/journal.pone.0031838.

**Berezin, A.**, 2011. A new plesiosaur of the Family Aristonectidae from the Early Cretaceous of the Center of the Russian Platform. Paleontological Journal 45: 648-660.

**Brown, B.**, 1913. A new plesiosaur, *Leurospondylus*, from the Edmonton Cretaceous of Alberta. Bulletin of the American Museum of Natural History 32: 605-615.

**Brown, D.S.**, 1981. The English Upper Jurassic Plesiosauroidea (Reptilia) and a review of the phylogeny and classification of the Plesiosauria. Bulletin of the British Museum (Natural History) Geology Series 35: 253-344.

**Carpenter, K.**, 1996. A review of short-necked plesiosaurs from the Cretaceous of the Western Interior, North America. Neues Jahrbuch für Geologie und Paläontologie Abhandlungen 201: 259-287.

**Cope, E.D.**, 1869. Synopsis of the extinct Batrachia, Reptilia and Aves of North America, Part 1. Transactions of the American Philosophical Society (new series) 14: 1-252.

**Cruickshank, A.R.I. & Fordyce, R.E.**, 2002. A new marine reptile (Sauropterygia) from New Zealand: further evidence for a Late Cretaceous austral radiation of cryptoclidid plesiosaurs. Palaeontology 45: 557-575.

**Cruickshank, A.R.I., Martill, D.M. & Noè, L.F.**, 1996. A pliosaur (Reptilia, Sauropterygia) exhibiting pachyostosis from the Middle Jurassic of England. Journal of the Geological Society 153: 873-879.

**de Blainville, H.D.**, 1835. Déscription de quelques espèces de reptiles de la Californie, précédée de l'analyse d'un système général d'Erpetologie et d'Amphibiologie. Nouvelles Annales du Muséum d'Histoire naturelle de Paris 3: 233-296.

**Druckenmiller, P.S. & Russell, A.P.**, 2006. A new elasmosaurid plesiosar (Reptilia: Sauropterygia) from the Lower Cretaceous Clearwater Formation, northeastern Alberta, Canada. Paludicola 5: 184-199.

**Druckenmiller, P.A. & Russell, A.P.**, 2008. Skeletal anatomy of an exceptionally complete specimen of a new genus of plesiosaur from the Early Cretaceous (Early Albian) of northeastern Alberta, Canada. Palaeontographica Abteilung A 283: 1-33.

**Gasparini, Z., Salgado, L. & Casadío, S.**, 2003. Maastrichtian plesiosaurs from northern Patagonia. Cretaceous Research 24: 157-170.

**Gasparini, Z., Salgado, L. & Parras, A.**, 2007. Late Cretaceous plesiosaurs from northern Patagonia, Argentina. Geological Journal 42: 185-202.

**Goloboff, P.A. & Farris, J.S.** 2001. Methods for quick Consensus estimation. Cladistics 17: S26-S34.

**Goloboff, P.A., Farris, J.S., Källersjö, M., Oxelman, B., Ramírez, M.J. & Szumika, C.A.**, 2003. Improvements to resampling measures of group support. Cladistics 19: 324-332.

**Goloboff, P.A., Farris, J.S. & Nixon, K.C.**, 2008. TNT, a free program for phylogenetic analysis. Cladistics 24: 774-786.

**Hiller, N., Mannering, A., Jones, C.M. & Cruickshank, A.R.I.**, 2005. The nature of *Mauisaurus haasti* Hector, 1874 (Reptilia: Plesiosauria). Journal of Vertebrate Paleontology 25: 588-601.

**Houssaye, A.**, 2009. 'Pachyostosis' in aquatic amniotes: a review. Integrative Zoology 4: 325-340.

**Ketchum, H.F. & Benson, R.B.J.**, 2010. Global interrelationships of Plesiosauria (Reptilia, Sauropterygia) and the pivotal role of taxon sampling in determining the outcome of phylogenetic analyses. Biological Reviews 85: 361-392.

**Ketchum, H.F. & Benson, R.B.J.**, 2011. A new pliosaurid (Sauropterygia, Plesiosauria) from the Oxford Clay Formation (Middle Jurassic, Callovian) of England: evidence for a gracile, longirostrine grade of early-middle Jurassic pliosaurids. Special Papers in Palaeontology 86: 109-129.

**Knutsen, E.M., Druckenmiller, P.S. & Hurum, J.H.**, 2012. Two new species of long-necked plesiosaurians (Reptilia: Sauropterygia) from the Upper Jurassic (Middle Volgian) Agardhfjellet Formation of central Spitsbergen. Norwegian Journal of Geology 92: 187-212.

**Mateus, O., Polcyn, M.J., Jacobs, L.L., Araújo, R., Schulp, A.S., Marinheiro, J., Pereira, B. & Vineyard, D.**, 2012. Cretaceous amniotes from Angola: dinosaurs, pterosaurs, mosasaurs, plesiosaurs, and turtles. V Jornadas Internacionales sobre Paleontología de Dinosaurios y su Entorno 71-105.

**O'Gorman, J.P., Gasparini, Z. & Salgado, L.**, 2014. Reappraisal of *Tuarangisaurus? cabazai* (Elasmosauridae, Plesiosauria) from the Upper Maastrichtian of northern Patagonia, Argentina. Cretaceous Research 47: 39-47.

**O'Keefe, F.R. & Chiappe, L.M.**, 2011. Viviparity and K-selected life history in a Mesozoic marine plesiosaur (Reptilia, Sauropterygia). Science 333: 870-873.

**O'Keefe, F.R. & Street, H.P.**, 2009. Osteology of the cryptocleidoid plesiosaur *Tatenectes laramiensis*, with comments on the taxonomic status of the Cimoliasauridae. Journal of Vertebrate Paleontology 29: 48-57.

**Otero, R.A., Soto-Acuña, S. & Rubilar-Rogers, D.**, 2012. A postcranial skeleton of an elasmosaurid plesiosaur from the Maastrichtian of central Chile, with comments on the affinities of Late Cretaceous plesiosauroids from the Weddellian Biogeographic Province. Cretaceous Research 37: 89-99.

**Owen, R.**, 1860. On the orders of fossil and recent Reptilia and their distribution in time. Report of the British Association for the Advancement of Science 29: 153-166.

**Sachs, S.**, 2004. Redescription of *Woolungasaurus glendowerensis* (Plesiosauria: Elasmosauridae) from the Lower Cretaceous of northeast Queensland. Memoirs of the Queensland Museum 49: 713-731.

**Sachs, S., Kear, B.P. & Everhart, M.J.**, 2013. Revised Vertebral Count in the 'Longest-Necked Vertebrate' *Elasmosaurus platyurus* Cope 1868, and Clarification of the Cervical-Dorsal Transition in Plesiosauria. PloS ONE 8(8): e70877.

**Sato, T.**, 2002. Description of plesiosaurs (Reptilia: Sauropterygia) from the Bearpaw Formation (Campanian-Maastrichtian) and a phylogenetic analysis of the Elasmosauridae. PhD dissertation, University of Calgary: 386 pp.

**Sato, T.**, 2003. *Terminonatator ponteixensis*, a new elasmosaur (Reptilia: Sauropterygia) from the Upper Cretaceous of Saskatchewan. Journal of Vertebrate Paleontology 23: 89-103.

**Sato, T.**, 2005. A new polycotylid plesiosaur (Reptilia: Sauropterygia) from the Upper Cretaceous Bearpaw Formation in Saskatchewan, Canada. Journal of Paleontology 79: 969-980.

**Sato, T. & Wu, X.-C.**, 2006. Review of plesiosaurians (Reptilia: Sauropterygia) from the upper Cretaceous Horseshoe Canyon Formation in Alberta, Canada. Paludicola 5: 150-169.

**Sato, T., Hasegawa, Y. & Manabe, M.** 2006. A new elasmosaurid plesiosaur from the Upper Cretaceous of Fukushima, Japan. Palaeontology 49: 467-484.

**Schwimmer, D.R., Stewart, J.D. & Williams, G.D.**, 1997. Scavenging by sharks of the genus *Squalicorax* in the Late Cretaceous of North America. Palaios 12: 71-83.

**Shimada, K., Tsuihiji, T., Sato, T. & Hasegawa, Y.**, 2010. A remarkable case of a shark bitten elasmosaurid plesiosaur. Journal of Vertebrate Paleontology 30: 592-597.

**Smith, A.S.**, 2007. Anatomy and systematics of the Rhomaleosauridae (Sauropterygia, Plesiosauria). PhD dissertation, University College, Dublin: 278 pp.

**Storrs, G.W.**, 1995. A juvenile specimen of *?Plesiosaurus* sp. from the Lias (Lower Jurassic, Pliensbachian) near Charmouth, Dorset, England. Proceedings of the Dorset Natural History and Archaeological Society 116: 71-76.

**Strganac, C., Jacobs, L.L., Ferguson, K.M., Polcyn, M.J., Mateus, O., Schulp, A.S., Morais, M.L. & Gonçalves, A.O.**, 2014. Carbon isotope events and $^{40}Ar/^{39}Ar$ age of the Cretaceous South Atlantic coast, Namibe Basin, Angola. Journal of African Earth Sciences 99: 452-462.

**Strganac, C., Jacobs, L.L., Polcyn, M.J., Mateus, O., Myers, T.S., Salminen, J., May, S.R., Araújo, R., Ferguson, K.M., Gonçalves, A.O., Morais, M.L., Schulp, A.S. & Tavares, T.S.**, 2015a. Geological setting and paleoecology of the Upper

Cretaceous Bench 19 Marine Vertebrate Bonebed at Bentiaba, Angola. Netherlands Journal of Geosciences.

*Strganac, C., Jacobs, L.L., Polcyn, M.J., Ferguson, K.M., Mateus, O., Gonçalves, A.O., Morais, M.L., Tavares, T. da S.*, 2015b. Stable oxygen isotope chemostratigraphy and paleotemperature regime of mosasaurs at Bentiaba, Angola. Netherlands Journal of Geosciences.

*Talevi, M. & Fernández, M.S.*, 2014. Remodelling of skeletal tissues bone and structural specialisations in an elasmosaurid (Sauropterygia: Plesiosauroidea) from the Upper Cretaceous of Patagonia, Argentina. Historical Biology. doi: 10.1080/08912963.2013.863882.

*Tumarkin-Deratzian, A.R., Vann, D.R. & Dodson, P.*, 2006. Bone surface texture as an ontogenetic indicator in long bones of the Canada goose *Branta canadensis* (Anseriformes: Anatidae). Zoological Journal of the Linnean Society 148: 133-168.

*Vincent, P. & Benson, R.B.G.*, 2012. *Anningasaura*, A basal plesiosaurian (Reptilia, Plesiosauria) from the Lower Jurassic of Lyme Regis, United Kingdom. Journal of Vertebrate Paleontology 32: 1049-1063.

*Vincent, P., Bardet, N. & Mattioli, E.*, 2012. A new pliosaurid from the Pliensbachian, Early Jurassic of Normandy, Northern France. Acta Palaeontologica Polonica 58: 471-485.

*Welles, S.P.*, 1943. Elasmosaurid plesiosaurs, with description of new material from California and Colorado. University of California, Memoirs 13: 125-254.

*Welles, S.P. & Bump, J.D.*, 1949. *Alzadasaurus pembertoni*, a new elasmosaur from the Upper Cretaceous of South Dakota. Journal of Paleontology 23: 521-535.

*Welles, S.P. & Gregg, D.R.*, 1971. Late Cretaceous marine reptiles of New Zealand. Records of the Canterbury Museum 9: 1-111.

*White, T.E.*, 1940. Holotype of *Plesiosaurus longirostris* Blake and classification of the Plesiosaurs. Journal of Paleontology 14: 451-467.

*Wiffen, J. & Moisley, W.L.*, 1986. Late Cretaceous reptiles (Families Elasmosauridae and Pliosauridae) from the Mangahouanga Stream, North Island, New Zealand. New Zealand Journal of Geology and Geophysics 29: 205-252.

*Wiffen, J., De Buffrénil, V., De Ricqlès, A. & Mazin, J.-M.*, 1995. Ontogenetic evolution of bone structure in Late Cretaceous Plesiosauria from New Zealand. Geobios 28: 625-640.

*Williston, S.W.*, 1903. North American Plesiosaurs. Field Columbian Museum, Geological Series 2: 1-16.

*Zinsmeister, W.J.*, 1979. Biogeographic significance of the late Mesozoic and early Tertiary molluscan faunas of Seymour Island (Antarctic Peninsula) to the final breakup of Gondwanaland. Ohio State University, Institute of Polar Studies (Eugene, OR): pp. 349-355.

## Appendix 1

Angolan/New Zealand/Argentine OTU0 ?????????????????????????????????????????????????????????????????????????????????????????????????????????????????????????????????????0101000000001?10000??11????????????0010320110[01]1?1011102521010439700000010001?00001?2?0?0??1?0?0

Angolan material ?????????????????????????????????????????????????????????????????????????????????????????????????????????????????????????????????????????????????????????????1111122320?200111111100011?11111?0?????????20????????1120000210?????????????????????0001??3200112300???????????????

New Zealand material ????????????????????????????????????????????????????????????????????????????????????????????????????????????????????????????????????????????????????1111122320?200111111100011?11111?0?????????20?1000100011200002l0???01??010210010 00??00001?032001123002?101?0[01]00??012?1

## Appendix 2

MONZ R1526 (Fig. 6): collected by A. McKay in 1873, Haumuri Bluff, South Island, New Zealand (Welles & Gregg, 1971). GNS CD 427, GNS CD 428 and GNS CD 429 (Fig. 7): collected by W.L. Moisley, T. Crabtree and M.A. Wiffen from the Mangahouanga stream, Hawke's Bay, North Island, New Zealand (Wiffen & Moisley, 1986). MML-Pv5: collected by D. Cabaza (Lamarque City, Río Negro Province), Locality C of Gasparini et al. (2003), Salinas de Trapalcó, Northern Patagonia, Argentina.